Real-Time Phase-Noise-Tolerant 2.5-Gb/s Synchronous 16-QAM Transmission

Ali Al-Bermani, Christian Wördehoff, Sebastian Hoffmann, David Sandel, Ulrich Rückert, and Reinhold Noé

***Abstract*—The 2.5-Gb/s coherent 16-quadrature amplitude modulation data is optically transmitted over 75 km and synchronously received by self-homodyning in a real-time in-phase and quadrature receiver, with bit-error ratio below forward-error correction threshold. To this purpose, a phase-noise-tolerant hardware-efficient feedforward carrier recovery was implemented.**

***Index Terms*—Coherent digital receiver, optical fiber communication, quadrature amplitude modulation (QAM), real-time systems, synchronous detection.**

I. Introduction

COHERENT optical transmission with high-order modulation formats permits a very efficient utilization of available fiber bandwidth together with a robustness against chromatic and polarization-mode dispersion (PMD). This is important for cost-efficient communication systems with channel rates of 112 Gb/s and above. In recent years, quadrature phase-shift keying (QPSK) was the preferred modulation format in research because of its robustness on long-haul links [1], [2]. But for transmission over less than ultimate distance, higher order quadrature amplitude modulation (QAM) is attractive, namely 16-point QAM which doubles spectral efficiency compared to QPSK. Simulations and off-line experiments have recently been published [3]–[5], but real-time investigations are essential for progress towards commercial application [6]–[8]. Based on our phase-noise-tolerant QAM carrier recovery algorithm [9], we present the implementation of a 16-QAM transmission system with a real-time synchronous demodulation and data recovery, reaching a data throughput of 2.5 Gb/s over 75 km.

II. Receiver Implementation Constraints

Real-time operation imposes constraints on coherent optical receivers: 1) Elaborate digital signal processors cannot be clocked at the same multigigabit/s rate as analog-to-digital converters (ADCs). Time-division demultiplexing is required and permits data processing, including synchronous carrier and data recovery, in M parallel modules at lower clock frequency. 2) Digital signal processing (DSP) must be implemented efficiently in hardware because complicated algorithms boost chip area, power consumption, and cost. The design should, therefore, not only be optimized by performance, but also by hardware aspects. 3) Feedback delay can hardly be tolerated. Carrier recovery by decision-feedback is impossible at multi-Gbaud symbol rate. Feedback loops must, therefore, be avoided in the carrier recovery process, especially for 16- and higher order QAM constellations where phase noise is very critical. Feedforward design is the method of choice.

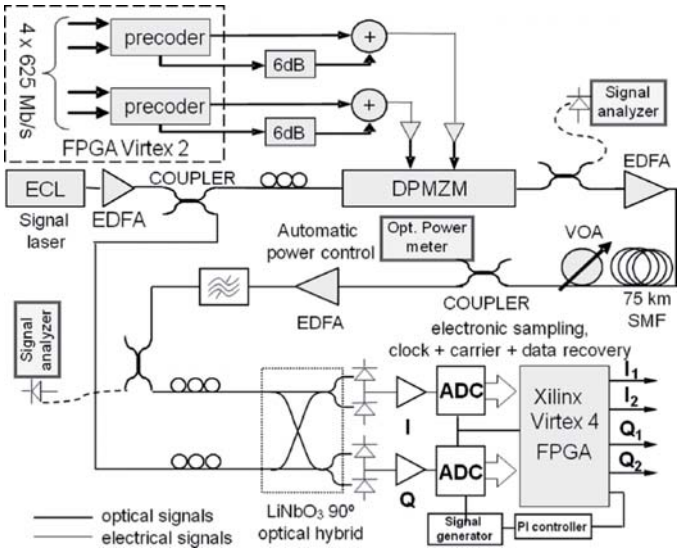

Fig. 1. Sixteen-QAM transmission setup with real-time synchronous coherent digital I&Q receiver.

III. Experimental Setup

Fig. 1 shows an optical 2.5-Gb/s transmission system, an improved version of our earlier setup [8]. Sixteen-QAM data is transmitted and detected in real-time. To resolve the fourfold ambiguity of the estimated optical phase within the receiver, the quadrant numbers of the in-phase (I) and quadrature (Q) data streams are modulo 4 differentially encoded. For 16-QAM data supply, two uncorrelated 625-Mbaud quaternary data streams are generated by a field-programmable gate array (FPGA), modulator drivers, attenuators, and resistive summers, as shown in Fig. 2. These drive a dual-parallel Mach–Zehnder modulator (DPMZM) consisting of two Mach–Zehnder interferometers (MZIs). An external cavity laser (ECL) is employed

Manuscript received July 28, 2010; revised October 06, 2010; accepted October 11, 2010. Date of publication October 18, 2010; date of current version November 24, 2010.

A. Al-Bermani, S. Hoffmann, D. Sandel, and R. Noé are with Optical Communication and High-Frequency Engineering, University of Paderborn, EIM-E, 33098 Paderborn, Germany (e-mail: Albermani@ont.uni-paderborn.de; Hoffmann@ont.uni-paderborn.de; Sandel@ont.uni-paderborn.de; noe@upb.de).

C. Wördehoff is with System and Circuit Technology, Heinz Nixdorf Institute, University of Paderborn, 33102 Paderborn, Germany (e-mail: cwoerdeh@hni.uni-paderborn.de).

U. Rückert is with the Center of Excellence–Cognitive Interaction Technology CITEC, Bielefeld University, D-33165 Bielefeld, Germany (e-mail: rueckert@techfak.uni-bielefeld.de).

Color versions of one or more of the figures in this letter are available online at http://ieeexplore.ieee.org.

Digital Object Identifier 10.1109/LPT.2010.2088385

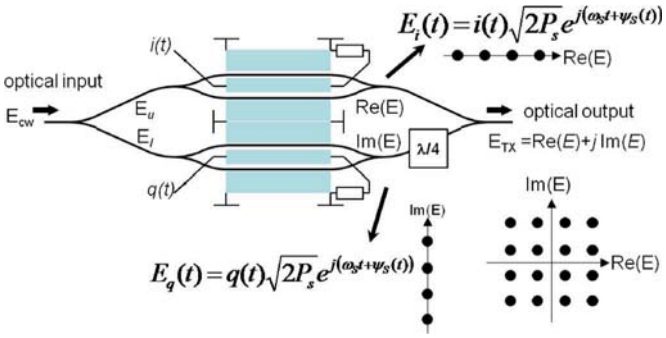

Fig. 2. Sixteen-QAM dual-parallel MZM simulated constellation diagram.

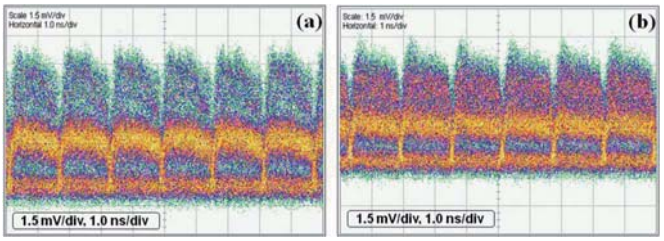

Fig. 3. (a) Intensity patterns of 625-Mbaud 16-QAM after DPMZM, and (b) after 75 km behind EDFA and filter for −20-dBm EDFA input power.

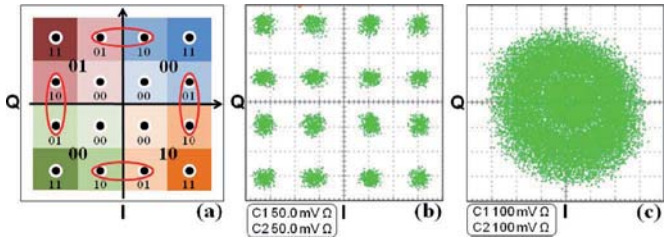

Fig. 4. (a) Sixteen-QAM coding. Large-font numbers (bits I_1, Q_1) denote quadrant, small-font numbers (bits I2, Q2) denote intraquadrant symbols. Due to differential quadrant encoding, encircled neighbor symbols differ by 2 bits, not by just 1 bit. (b) Constellation in the transmitter and (c) after optical transmission for −20-dBm preamplifier input power.

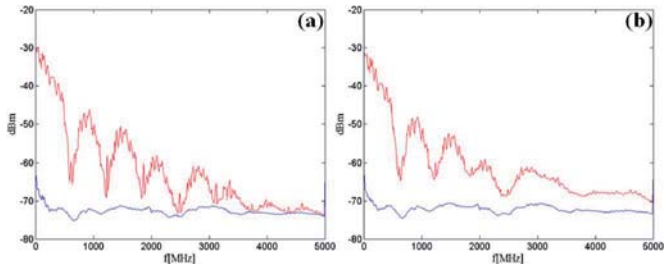

Fig. 5. Electrical spectra in one quadrature with either aligned (top) or orthogonal (bottom) signal and LO polarizations, showing signal and noise, for (a) −20 dBm and (b) −45-dBm preamplifier input power.

in a self-homodyne arrangement (150-kHz specified linewidth, 1.5-dBm output power).

The ECL signal passes an erbium-doped fiber amplifier (EDFA) and is split. One signal portion is fed into the DPMZM for transmission (TX) while the other portion replaces the local oscillator (LO) laser for coherent reception. The fiber launch power at the TX-EDFA output is −1.5 dBm. After transmission through 75 km of standard single-mode fiber, the signal is fed into a variable optical attenuator (VOA), followed by an EDFA and a ∼20-GHz-wide bandpass filter for noise filtering. In Fig. 3, the optical signal before (a) and after (b) transmission is plotted, as measured in an oscilloscope with attached photodiode, cf., also Fig. 1. The unequal amplitudes are due to different pump powers applied to the EDFA.

Polarization is controlled manually. TX and LO signals are superimposed in a $LiNbO_3$ 90° optical hybrid and detected in two differential photodiode pairs. The electrical I&Q signal components are amplified before being sampled in two 6-bit ADCs at the symbol rate of 625 MHz. For clock recovery, we use a second time-interleaved ADC pair (not shown) to provide the required oversampling. The ADCs interface with a Xilinx Virtex 4 FPGA where carrier and data are recovered electronically. To obtain a clock phase error signal the signs of adjacent input samples are correlated [1], [10] and fed out to an external PI controller which controls a voltage-controlled oscillator and closes a phase-locked loop. For carrier recovery, the primary received I&Q samples are combined as a symbol pointer in the complex plane and rotated into the first quadrant. Then they are rotated within the quadrant in parallel by $B = 16$ test carrier phase angles [9]. The squared distance between the recovered 16-QAM symbol and the closest constellation point is filtered over $2N + 1$ consecutive symbols. That test phase angle where the filtered squared distance is minimum yields the correct constellation point within a quadrant, i.e., data bits I_2, Q_2. Data bits I_1, Q_1 are obtained through differential modulo 4 decoding of the quadrant number. This prevents occurring quadrant phase jumps of the recovered carrier from falsifying all subsequent data, but results in some deviations from ideal Gray coding, cf., Fig. 4(a). Digital signal processing takes place in $M = 8$ demultiplexed parallel streams, thereby reducing the internal clock frequency to 78.125 MHz. The carrier recovery does not contain any feedback loop, so it can be adapted to any transmission rate by increasing M. The optimum response halfwidth N of the squared-distance filter depends on the laser-sum-linewidth-times-symbol-interval-product $\Delta f \cdot T$; we chose $N = 6$ for this experiment, which value worked best. For bit-error-ratio (BER) measurement, appropriate patterns are programmed into the BER tester.

While the hardware effort for carrier recovery is on the order of $B = 16$ times larger than for QPSK, capacity is all the same doubled. Also, equalizers typically consume much more silicon floorspace than QPSK carrier recoveries. In the future, a two-stage version [11] of the implemented concept could reduce hardware effort further.

IV. Measurement Results

Electrical data transmission was error-free. Fig. 4 shows the electrical constellation diagram in the transmitter (b) and after optical transmission over 75 km of fiber for −20-dBm preamplifier input power (c). An SNR of 35 dB was measured at one ADC input, using electrical noise power in a 312.5-MHz band and total electrical signal power. Corresponding spectra are shown in Fig. 5.

Fig. 6 shows BER versus received power for 2.5-Gb/s transmission over distances of 5.5 and 75 km, using $2^7 - 1$ PRBS data. Clock was either supplied directly from the transmitter,

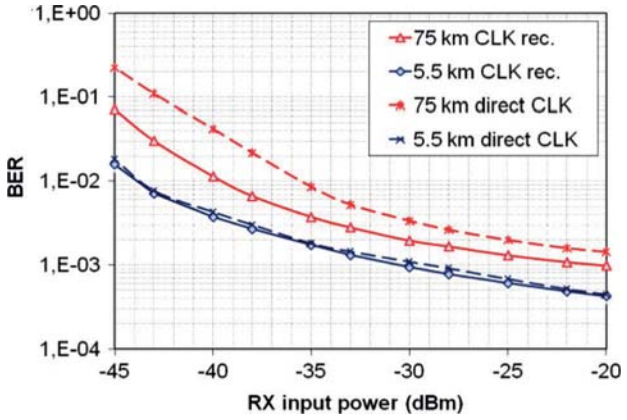

Fig. 6. Measured BER versus optical power at the preamplifier input, averaged over all four subchannels (I1, Q1, I2, and Q2) at 2.5-Gb/s data rate.

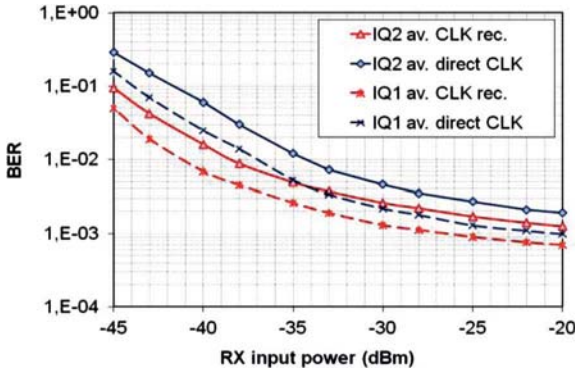

Fig. 7. Measured BERs of 16-QAM bits 1 and 2, each averaged over I&Q, versus optical power at preamplifier input. Fiber length was 75 km.

or recovered in the receiver. The BER deviations between the receiver setups with and without clock recovery show the influence of timing jitter depending on transmission distance. The best measured BERs were at $4.47 \cdot 10^{-4}$ and $4.2 \cdot 10^{-4}$ for 5.5 km, and $1.45 \cdot 10^{-3}$ and $9.75 \cdot 10^{-4}$ for 75 km of fiber, for direct clock and clock recovery, respectively. All measurements were repeated several times and turned out to be stable. The total capacity of the conducted 625-Mbaud experiment is 4×625 Mb/s or 2.5 Gb/s.

Fig. 7 shows measured BERs versus preamplifier input power, averaged over I&Q but separate for interquadrant bits (IQ1), Gray-encoded as in [9], and intraquadrant bits (IQ2). Distance was 75 km. Intraquadrant decoding is limited more strongly than interquadrant decoding, presumably by intersymbol interference (ISI) in the nonideal electrical transmitter. This is seen from the fact that the BER of I_2 and Q_2 (inside quadrant) is higher than the BER of the quadrant numbers I_1 and Q_1. Based on simulations without ISI we estimated the BER floor to be ideally at 10^{-4} for our $\Delta f \cdot T = 0.00048$. Averaged over all four subchannels (I_1, Q_1, I_2, and Q_2) at received powers larger than -30 dBm, the measured BER was all the same less than a forward-error correction (FEC) limit $(2 \cdot 10^{-3})$. We did not use FEC. According to simulation, the experimental response halfwidth $N = 6$ of the carrier recovery is optimum for a single-polarization 16-QAM system with good receiver sensitivity and phase noise tolerance. This is important because a high received power would always tolerate much phase noise, simply by lowering N. The implemented carrier recovery algorithm is compatible with all kinds of equalizers for polarization control, chromatic dispersion (CD), and PMD.

V. Summary

We demonstrated a real-time 16-QAM transmission system with a digital receiver for synchronous carrier and data recovery. The 2.5-Gb/s 16-QAM data (625 Mbaud) was transmitted over 75 km of fiber in a self-homodyne configuration with an ECL. The averaged BER was below the threshold of a state-of-the-art FEC for receiver input powers above -30 dBm.

Acknowledgment

The authors would like to thank T. Pfau for his earlier contributions to this experiment.

References

[1] T. Pfau *et al.*, "First real-time data recovery for synchronous QPSK transmission with standard DFB lasers," *IEEE Photon. Technol. Lett.*, vol. 18, no. 18, pp. 1907–1909, Sep. 15, 2006.

[2] H. Sun, K. Wu, and K. Roberts, "Real-time measurements of a 40 Gb/s coherent system," *Opt. Express*, vol. 16, pp. 873–879, 2008.

[3] L. Molle, M. Seimetz, D. Gross, R. Freund, and M. Rohde, "Polarization multiplexed 20 Gbaud square 16 QAM long-haul transmission over 1120 km using EDFA amplification," presented at the ECOC 2009, Vienna, Austria, Sep. 20–24, 2009, Paper We 8.4.4, .

[4] A. H. Gnauck and P. J. Winzer, "10 × 112-Gb/s PDM 16-QAM transmission over 1022 km of SSMF with a spectral efficiency of 4.1 b/s/Hz and no optical filtering," presented at the ECOC 2009, Vienna, Austria, Sep. 20–24, 2009, Paper We 8.4.4.

[5] I. Fatadin, D. Ives, and S. J. Savory, "Blind equalization and carrier phase recovery in a 16-QAM optical coherent system," *J. Lightw. Technol.*, vol. 27, no. 15, pp. 3042–3049, Aug. 1, 2009.

[6] T. Pfau *et al.*, "Coherent optical communication: Towards realtime systems at 40 Gbit/s and beyond," *Opt. Express*, vol. 16, pp. 866–872, 2008.

[7] M. Nakamura, Y. Kamio, and T. Miyazaki, "Real-time 40-Gbit/s 16-QAM self-homodyne using a polarization-multiplexed pilot-carrier," in *Proc. IEEE/LEOS Summer Topical Meetings*, Acapulco, 2008, pp. 14.15–14.30, Paper WC2.3.

[8] A. Al-Bermani *et al.*, "Realtime 16-QAM transmission with coherent digital receiver," in *Proc. IEEE OECC 2010*, Sapporo, Japan, Jul. 5–9, 2010, (7B4-2).

[9] T. Pfau, S. Hoffmann, and R. Noé, "Hardware-efficient coherent digital receiver concept with feedforward carrier recovery for M-QAM constellations," *J. Lightw. Technol.*, vol. 27, no. 8, pp. 989–999, Apr. 15, 2009.

[10] F. Gardner, "A BPSK/QPSK timing-error detector for sampled receivers," *IEEE Trans. Commun.*, vol. 34, no. 5, pp. 423–429, May 1986.

[11] T. Pfau and R. Noé, "Phase-noise-tolerant two-stage carrier recovery concept for higher order QAM formats," *IEEE J. Sel. Topics Quantum Electron.*, vol. 16, no. 5, pp. 1210–1216, Sep./Oct. 2010.